Overview and analysis of optical sensing techniques over deployed telecom networks

Overview and analysis of optical sensing techniques over deployed telecom networks

Ann Margareth Rosa Brusin[1], Giuseppe Rizzelli[1], Marco Fasano[2], Jacopo Morosi[3], Saverio Pellegrini[1], Valter Ferrero[1], Gabriella Bosco[1], Dario Pilori[1], Paola Parolari[2], Andrea Madaschi[2], Marco Brunero[3], Pierpaolo Boffi[2] and Roberto Gaudino[1]

[1]*Politecnico di Torino, Italy* [2]*Politecnico di Milano, Italy* [3]*COHAERENTIA, Italy*

e-mail: giuseppe.rizzelli@polito.it

ABSTRACT In this Invited Paper, we review the most promising techniques that have been recently proposed for optical sensing over deployed telco fiber networks, with a particular emphasis on methods that allow coexistence with telco traffic (typically using a WDM approach). For the most promising solutions, physical layer simulations and experiments are presented to further elaborate on coexistence constraints.

1. Introduction

The use of distributed optical fiber sensing is today well established in some specific fields (such as oil/gas pipeline monitoring over long distances) but most of these applications use dedicated fibers and, usually, also specific installation procedures [1]. Optical fibers are today ubiquitously deployed worldwide for telco high speed data transmission for both transport networks over long distances and for metro and access optical networking solutions inside any urban areas. Several research groups [2], [3], [4], [5] have recently reported preliminary demonstrations of the novel idea of re-using deployed telco fibers for distributed sensing applications alongside data transmission. This is (in principle) possible using Wavelength Division Multiplexing (WDM), dedicating a portion of the available optical spectrum to traditional data transmission and another to the optical sensing signal. If techno-economically successful, this novel paradigm would enable extensive and geographically distributed monitoring capabilities in any deployed areas of the world, with applications to earthquake and catastrophic geological event detection, early warning of fiber cuts due to construction works or several other potentially dangerous events happening alongside deployed optical fibers.

In the following, we provide a classification and analysis of these solutions, assessing the physical layer compatibility between various optical sensing techniques and data transmission on the same fiber. The paper is organized as follows: in Sect. 2 we present a taxonomy of different sensing solutions and some preliminary considerations on their compatibility with data transmission in terms of spectral occupation and generation of mutual nonlinear interference. Then, we present some physical layer simulations on interferometric sensing (Sect. 3) and experiments on Distributed Acoustic Sensing (DAS) (Sect. 4) coexisting with data transmission.

2. A Taxonomy of Optical Sensing Options on Deployed Telco Fiber networks

In order to discuss the pros and cons of different sensing technologies, we present in Table I an overview of various sensing technologies, detailing their primary characteristics and their compatibility with WDM traffic sharing the same fiber. We discuss in particular the importance of two critical factors in determining coexistence feasibility: the optical bandwidth demands of the sensing system and the potential nonlinear cross-talk between the sensing signal and telco wavelengths, and vice versa. For the various sensing techniques reported in Table I, we observe that:

1) Raman-based solutions are based on the detection of the anti-Stokes induced signal, spaced about 13 THz from the pulsed pump. Coexistence with the telecom data requires precise wavelength positioning in the WDM spectrum, avoiding proximity to the pump due to the nonlinear Kerr effect and ensuring sufficient separation from the very weak anti-Stokes sensing signal. Two completely different optical bands could be used, such as the C-band for Raman sensing and the O-band for data transmission (or vice-versa).
2) Interferometric-based solutions require very limited optical bandwidth, since the sensing laser is usually not modulated. Additionally, as shown by simulations in the next section, they are not limited by Kerr-induced nonlinear cross-talk for the power levels of interest. Consequently, they potentially enable a straightforward coexistence between data and sensing signals [6], [7], [8] .
3) Brillouin-based and DAS solutions require relatively narrow optical bandwidth allocated for sensing, certainly less than the typical 50-100 GHz spacing used for DWDM data transmission. However, the physical layer compatibility can be limited by fiber Kerr nonlinear effects due to the high peak power pulses that are generated by the sensing system. Compatibility should thus be studied case by case, as we preliminary show in the next sections.

In Table I, we also report an alternative solution based on monitoring the state of polarization (SOP) using the internal DSP information available "for free" in coherent receivers [9]. This solution is fully compatible with data transmission, as the PM-QAM modulated data signal is used also for sensing. However, contrary to the

979-8-3503-7732-3/24/$31.00

	RAMAN sensing	BRILLOUIN sensing	Distributed acoustic sensing (DAS)	Ultra-stable laser interferometry	In-cable Michelson interferometry	State of Polarization in coherent transceivers
Required Back-propagation	YES	YES	YES	YES or loop scheme	YES or loop scheme	NO
Typical response time	Slow (tens of seconds)	Slow (tens of seconds)	Fast (milliseconds)	Fast (microseconds)	Fast (microseconds)	Fast (microseconds)
Max distance	Tens of km	Tens of km	Up to 100 km	Thousands of km	Tens of km	Thousands of km
Spatial resolution	1 m	< 1 m	0.1 m	Requested multiple detection for localization	Requested multiple detection for localization	NO spatial resolution
Temperature measurement	YES	YES	Not used	Not used	Not used	Not used
Strain measurement	Not used	YES	YES	YES	YES	Yes, but only qualitative
Typical power for the optical source	2 W peak	500 mW peak	1 W peak	100 mW CW	10 mW CW	Tens of mW (CW, not pulsed)
Laser linewidth	~MHz	~MHz	~kHz	~Hz	~MHz	~100 kHz
Required Optical bandwidth	f_{laser}±13 THz	f_{laser}±11 GHz	(in principle) Same as laser linewidth	(in principle) Same as laser linewidth	(in principle) Same as laser linewidth	Same as PM-QAM transmission
Compatibility with DWDM on deployed optical networks	NO Required spectrum and power are too large	In principle, these sensing solutions are spectrally compatible with telco fiber transmission (they use an optical bandwidth equal or smaller than the DWDM channel one)				Fully compliant
		Brillouin and DAS require very high peak power, so that the actual compatibility in terms of signal crosstalk is anyway to be carefully studied case by case		Interferometry usually requires lower power and it has already been demonstrated to have negligible impact on DWDM traffic		

TABLE I: *A comparison of possible sensing techniques over deployed optical fiber network.*

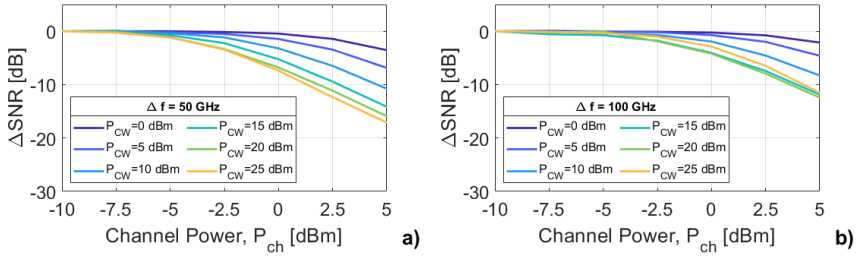

Figure 1: *Interferometric scenario: ΔSNR for sensing channel vs. channel power P_{ch} for different CW laser power P_{CW} for a) 50 GHz and b) 100 GHz channel frequency spacing.*

other solutions, it does not allow localization of the anomalous events hitting the fiber, since it is based on the SOP "length-integrated" time-variations.

3. Simulations to assess physical layer compatibility for interferometric solutions

In this Section, we analyze through simulations the coexistence of a sensing signal based on interferometric techniques [6]-[7] which co-propagates with WDM data traffic traveling along the same fiber, presenting preliminary results obtained through time-domain simulations exploiting the split-step Fourier method (SSFM) [10] to investigate possible Kerr nonlinear effects. We focus on single span solutions, such as links between two amplifiers or non-amplified systems. The simulation setup consists of 11 channels in the ITU-T WDM grid centered at 193.4 THz (channels numbered from 1 to 11), assuming two different channel spacings Δf=50 GHz or 100 GHz, 32 GBaud PM-16QAM modulation format and typical SRRC shaping (with roll-off=0.15). The sensing probe signal is assumed to be a CW laser with 100 kHz linewidth (Wiener phase noise model) placed on the central channel of the WDM comb (channel 6). The link is composed of a single 100 km SMF fiber span (α=0.2 dB/km, D=+17 ps/nm/km, Kerr non-linear coefficient γ=1.3 1/W/km and PMD=0.05 $\mathrm{ps}/\sqrt{\mathrm{km}}$). An EDFA ($G$=20 dB, NF=5 dB) is inserted at the end of the fiber to fully recover for the propagation loss. To mimic the presence of the noise generated while propagating along multiple fiber spans, we insert an additive white Gaussian noise source to set the received optical signal-to-noise ratio (OSNR) to 14.3 dB, corresponding to BER$\simeq 10^{-2}$. At the receiver side, after the wavelength demultiplexer, standard coherent digital signal processing (DSP) is applied to data channels, including optical filtering, chromatic dispersion compensation, adaptive equalization and carrier phase recovery. Instead, the sensing signal is first filtered by a 4^{th}-order Super-Gaussian optical filter with 5 GHz cut-off frequency, then detected by a photodiode and further filtered by a 4^{th}-order Butterworth filter with 5 GHz cut-off frequency. On both signals we assess the SNR level.

To focus on the potential cross-talk generated by fiber Kerr nonlinear effects, we simulated different power levels for the data (P_{ch} $\in$[-10,5] dBm) and the CW sensing signal (P_{CW} $\in$[0,25] dBm). The impact of data traffic on the sensing signal is shown in Figs. 1a and 1b in terms of SNR penalty (ΔSNR) across various P_{ch} values (for 50 GHz and 100 GHz spacing). Specifically, the ΔSNRs were normalized to the SNR computed for P_{ch}=-10 dBm at the respective P_{CW}. As expected, the impact of data channels on the sensing signal is less pronounced when the channel spacing is 100 GHz, as the channels are further apart, thus generating a reduced cross-phase modulation (XPM) [11]. In general, we can observe that, when the laser power is low (P_{CW}=0 dBm), the impact of data traffic on the sensing signal is limited, also when the channel power reaches

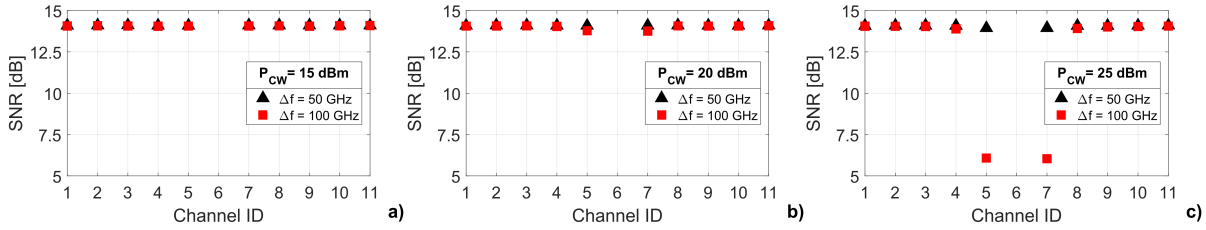

Figure 2: *SNR of WDM data channels with power P_{ch}=0 dBm for three different CW laser powers: a) P_{CW}=15 dBm, b) P_{CW}=20 dBm and c) P_{CW}=25 dBm.*

5 dBm: -3.5 dB and -2.0 dB of ΔSNR is experienced for Δf=50 GHz and Δf=100 GHz, respectively. However, when the laser power increases, larger SNR degration is observed at higher channel power, especially when P_{ch} >-2.5 dBm. Additionally, the ΔSNR vs P_{ch} curves tend to saturate for increasing laser power, as the effects generated by a higher channel power are overcome by stronger nonlinearities generated on the sensing signal.

Fig. 2 shows the impact of the sensing signal on data channels at P_{ch}=0 dBm for both channel spacing values and P_{CW}= 15 dBm, 20 dBm or 25 dBm. For 100 GHz spacing, no considerable SNR decrease is noticed, while this is no longer true with 50 GHz spacing. Indeed, at P_{CW}=20 dBm we start to see a slight impact on channels 5 and 7, and this effect becomes particularly significant at P_{CW}=25 dBm, where the SNR reduces to 6 dB.

From simulation results, we can conclude that, for interferometric sensing techniques such as those presented in [6]-[7], coexistence on the same fiber between DWDM data traffic and interferometric sensing signals should not be a problem for the typical power levels of interest, i.e. for P_{ch} around 0 dBm and for P_{CW} up to ∼20 dBm.

4. Preliminary Experiments to Assess Physical Layer Compatibility for DAS Solutions

In this Section, we present a preliminary experimental analysis of the coexistence between a sensing signal based on the DAS technique and WDM data traffic co-propagating on the same deployed underground optical fiber. The experimental setup is shown in Fig. 3a. A commercial coherent transceiver is used to transmit and receive a channel under test (CUT) at 193.3 THz on channel number 33 of the ITU-T WDM grid, carrying a 32 GBaud PM-16QAM modulation format (200 Gbps net bit rate). The WDM comb is obtained by combining the modulated signal with other 28 dummy channels spaced by 100 GHz generated through proper shaping of an amplified spontaneous emission (ASE) source. A second coupler is used to add ASE noise and set a specific OSNR level to the WDM channels through noise loading based on an EDFA for ASE generation, an optical filter and a variable optical attenuator (VOA). A third optical coupler is used to insert the DAS pulsed signal at 193.4 THz in the channel 34 slot of the ITU-T grid. The DAS signal is generated by a commercial device. The whole comb is then launched on ∼11.8 km SMF fiber deployed underground in a urban environment (Turin, Italy city center) with both termination located in our PhotoNext laboratory. Upon returning in our lab, the signal is perturbed by means of a cylindrical piezo-transducer (PZT) driven by an arbitrary waveform generator (AWG). Specifically, it produces a 23 Hz vibration with 2 V peak-to-peak amplitude on about few meters of 900 μm tight fiber patchcord wrapped around the PZT. Fig. 3b shows the waterfall plot of a 55 s duration DAS measurement performed on the metro fiber link in case of sensing signal power P_s=29 dBm. There, multiple vibration effects can be observed in the time-distance domain, which is somehow expected on a fiber buried underneath a mid-sized city like Turin, where human activities are very intense during the day. To better visualize the PZT induced 23 Hz vibration, a zoom around the fiber link termination is provided in the inset of Fig. 3b. In Fig. 3c, the time domain evolution of the strain rate over a 2 s timescale is reported.

The characterization of the mutual effect between the DAS sensing signal and the data signal has been performed in different scenarios. The results are shown in Fig. 4. The DAS emits a pulsed signal with 50 ns duration and 1 kHz repetition rate with variable pulse peak power P_s. To test different levels of nonlinear Kerr effects, different peak power levels (P_s ∈[17,29] dBm) were set after the third coupler, before entering the metropolitan fiber. Instead, the PM-16QAM 32 Gbaud data signal had -4 dBm average power at the fiber input, resulting in ∼10.5 dBm overall average optical power for the 28-channel WDM comb. Fig. 4a shows the SNR

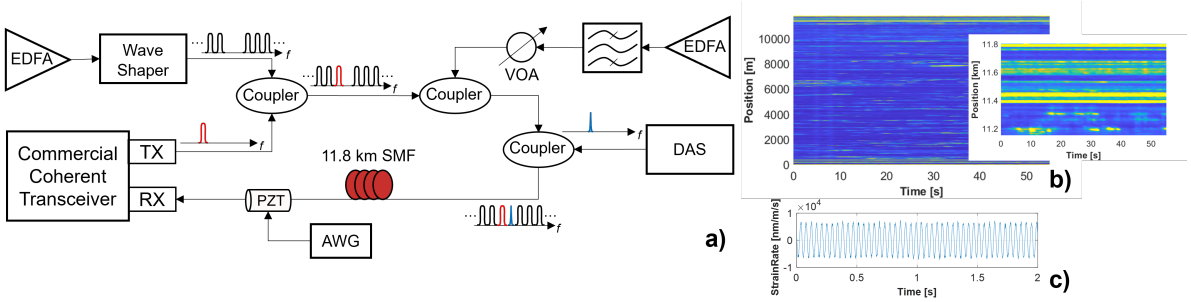

Figure 3: *a) Experimental setup, b) waterfall plot of the DAS measurement, and c) strain rate evolution in time.*

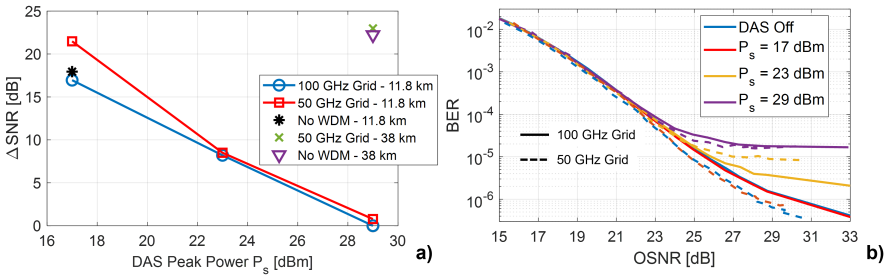

Figure 4: *a) ΔSNR of the DAS received signal. b) BER vs OSNR measured on the data channel under test for different DAS peak power values assuming 100 GHz (solid) and 50 GHz (dashed) grids and 11.8 km fiber.*

penalty (ΔSNR) on the DAS received signal, as a function of peak power P_s for different data traffic conditions: 100 GHz and 50 GHz spacings with 11.8 km fiber, and 50 GHz spacing with 38 km fiber. For reference, also scenarios with no data traffic are reported. In particular, to determine the ΔSNR, we compute the SNR on a 2 s time window, which we then normalize to the lowest value obtained for P_s=29 dBm in case of 100 GHz spacing and propagation over the 11.8 km fiber. When the grid spacing is reduced to 50 GHz, no impact is observed on the SNR at high DAS peak power, whereas the SNR penalty is much higher (also with respect to the case without WDM traffic, black marker) for a relatively low sensing signal power (P_s=17 dBm): the modulated telco signal degrades the quality of the DAS signal by ∼4 dB.

The impact on the sensing signal over the 38 km link was studied only at the highest DAS peak power (P_s=29 dBm), as the DAS was not able to detect perturbations at lower powers. The obtained results confirm a good coexistence capability, as data traffic does not affect the DAS sensitivity. Moreover, as depicted in Fig. 4b, where the pre-FEC BER is plotted as a function of the OSNR, the impact of the DAS signal on the data transmission system for the 11.8 km link is only visible at very low BER levels. Indeed, regardless of the DAS peak power and for BER down to 10^{-4}, the BER curves are perfectly superimposed for both spectral spacing, whereas at lower BER, an increasing degradation can be observed for increasing P_s.

5. Conclusions

We have addressed compatibility between data transmission and optical sensing techniques on the same fiber, showing that this is a compelling and emerging research domain that demands further investigation and development. Our focus was only on physical layer limitations for DAS and interferometric sensing techniques, but clearly techno-economics analysis is also a key topic, given the current high costs associated with traditional distributed sensing hardware, in view of a potential widespread use on the enormous set of deployed telco fibers.

ACKNOWLEDGMENTS A. M. Rosa Brusin, G. Bosco, M. Fasano and P. Boffi are sponsored by the European Union under the Italian National Recovery and Resilience Plan (NRRP) of NextGenerationEU, partnership on 'Telecommunications of the Future' (PE00000001 - program 'RESTART'). G. Rizzelli, V. Ferrero, S. Pellegrini, P. Parolari and R. Gaudino are sponsored by the SURENET project – funded by European Union – Next Generation EU within the PRIN 2022 program (D.D. 104 - 02/02/2022 Ministero dell'Università e della Ricerca). This manuscript reflects only the authors' views and opinions and the Ministry cannot be considered responsible for them.

REFERENCES

[1] A. Lellouch, and B. L. Biondi, "Seismic Applications of Downhole DAS", *Sensors*, vol. 21, no. 9, 2021.
[2] A. Mecozzi, C. Antonelli, M. Mazur, N. Fontaine, H. Chen, L. Dallachiesa, R. Ryf, "Use of Optical Coherent Detection for Environmental Sensing," *J. Lightw. Technol.*, vol. 41, no. 11, pp. 3350-3357, 2023.
[3] E. Ip, Y. Huang, G. Wellbrock, T. Xia; M.; T. Wang; Y. Aono, "Vibration Detection and Localization Using Modified Digital Coherent Telecom Transponders," *J. Lightw. Technol.*, vol. 40, no. 5, pp. 1472-1482, 2022.
[4] P. Boffi, M. Brunero, M. Fasano, A. Madaschi, J. Morosi, A. Gatto, M. Ferrario, "Real-Time Surveillance of Rail Integrity by the Deployed Telecom Fiber Infrastructure," *IEEE Sensors Journal*, vol. 23, no. 21, pp. 26012-26021, 2023.
[5] S. Pellegrini, L. Minelli, L. Andrenacci, D. Pilori, G. Bosco, B. Koch, R. Noé, C. Crognale, S. Piciaccia, R. Gaudino "Real-Time Demonstration of Anomalous Vibrations Detection in a Metro-like Environment using a SOP-based Algorithm," in *Proc. of Optical Fibers Communications (OFC) Conference*, San Diego, 2024.
[6] I. Di Luch, M. Ferrario, P. Boffi, G. Rizzelli, H. Wang and R. Gaudino, "Demonstration of structural vibration sensing in a deployed PON infrastructure," in *Proc. of European Conference on Optical Communication (ECOC)*, Dublin, Ireland, 2019, pp. 1-3.
[7] I. Di Luch, M. Ferrarlo, G. Rizzelli, R. Gaudino and P. Boffi, "Vibration Sensing for Deployed Metropolitan Fiber Infrastructures," in *Proc. of Optical Fiber Communications Conference and Exhibition (OFC)*, San Diego, CA, USA, 2020, pp. 1-3.
[8] I. D. Luch, P. Boffi, M. Ferrario, G. Rizzelli, R. Gaudino and M. Martinelli, "Vibration Sensing for Deployed Metropolitan Fiber Infrastructure," *Journal of Lightwave Technology*, vol. 39, no. 4, pp. 1204-1211, 2021.
[9] S. Pellegrini, L. Andrenacci, L. Minelli, D. Pilori, G. Bosco, L. Della Chiesa, R. Gaudino, "Estimation Accuracy of Polarization State from Coherent Receivers for Sensing Applications," in *Proc. of 2023 IEEE Photonics Conference (IPC)*, Orlando, FL, USA, 2023, pp. 1-2.
[10] D. Pilori, M. Cantono, A. Carena and V. Curri, "FFSS: The fast fiber simulator software," 2017 19th International Conference on Transparent Optical Networks (ICTON), Girona, Spain, 2017, pp. 1-4.
[11] R. Dar, M. Feder, A. Mecozzi and M. Shtaif, "Pulse Collision Picture of Inter-Channel Nonlinear Interference in Fiber-Optic Communications," *J. Lightw. Technol.*, vol. 34, no. 2, pp. 593-607, 2016.